Int. J. Electrochem. Sci., 11 **(2016)** 10320 – 10328, doi: 10.20964/2016.12.66

International Journal of
ELECTROCHEMICAL
SCIENCE
www.electrochemsci.org

Short Communication

Organometal Halide Perovskite $CH_3NH_3PbI_3$ as an Effective Photosensitizer for p-Type Solar Cells

Jie Qu[1,*], *Wenchang Wang*[1], *Jia Cheng*[2], *Shuai Zhang*[1], *Jianning Ding*[1,*], *Ningyi Yuan* [1]

[1] School of Materials Science and Engineering, Jiangsu Collaborative Innovation Center of Photovoltaic Science and Engineering and Jiangsu Province Cultivation base for State Key Laboratory of Photovoltaic Science and Technology, Changzhou University, Changzhou 213164, P. R. China
[2] Hunan Hua Teng Pharmaceutical Co., Ltd, Changsha 410205, P. R. China
[*]E-mail: qujie1981@cczu.edu.cn, dingjn@cczu.edu.cn

Received: 12 September 2016 / *Accepted:* 19 October 2016 / *Published:* 10 November 2016

$CH_3NH_3PbI_3$ sensitizers are prepared with different mixed solvents. Using butyrrolactone/dimethyl sulphoxide mixed solvent, a smooth film with roughness of 12 nm is obtained. The prepared $CH_3NH_3PbI_3$ are used as photosensitizers of p-DSSC. Photoelectrical performance indicates that $CH_3NH_3PbI_3$ with butyrrolactone/dimethyl sulphoxide presents a higher J_{sc} of 7.5 mA cm^{-2} and a higher efficiency of 0.53%, which may contribute to its improved UV-vis absorption and smooth film. Researches further indicate that $CH_3NH_3PbI_3$ with butyrrolactone/dimethyl sulphoxide provides fast hole transport, less recombination and improved hole collection efficiency.

Keywords: p-type solar cells; perovskite; photocathode; photoelectrical performance

1. INTRODUCTION

In 2000, the first tandem solar cells consisted of a dye-sensitized photoanode and dye-sensitized photocathode were rerported [1], it is well suggested to improve its performance through enhancing the photo-conversion efficiency. However, the over all efficiency is limited by its low current and voltage on the p-side. The best performance of p-DSSC was reported by U. Bach, which indicated a conversion efficiency of 1.3 % [2]. Therefore, how to improve the photoelectrical performance of p-DSSC became an urgent thing to prepare effective tandem solar cells [3-10]. To improve the intrinsically low open circuit voltage V_{oc} (0.1V), one method is to prepare different semiconductors to enlarge the potential between the quasi-Fermi level in the semiconductor and the electrochemical potential of the redox mediator [3-5]. Another efficitive way to improve photocurrent

is to design high efficient sensitizer with a broad absorption range of the solar spectrum and a matched bandgap energies for facilitating higher hole injection efficiency [6-10].

Many efforts have been made to synthesize new photosensitizers, including coumarin [11-14], perylene monoimide [15-16] and porphyrin [17]. No significant improvement was achieved until "donor-acceptor" type dye was synthesized. Such dyes with anchoring group on the triphenylamine donor show high incident photon-to-electron conversion efficiency (IPCE) and significant improved photocurrent density (J_{sc}) [18-19]. Another excellent work was done by Bauerle and Bach et al [20]. Oligothiophene with tunable length was used as donor units. Such dyes exhibit long-lived charge separated excited states which could reduce the fast charge recombination. The efficiency of absorbed photons to electrons can reach up to 96%, resulting in a great increase in energy conversion efficiency. Besides, other soalr dyes have also been applied to replace organic dyes such as quantum dots (QDs) and perovskites [6, 10].

In this article, $CH_3NH_3PbI_3$ sensitizers are prepared with different mixed solvents, dimethylacetamide/dimethylformamide (DMAC/DMF) and butyrrolactone/dimethyl sulphoxide (BL/DMSO). The quality of the $CH_3NH_3PbI_3$ film is affected by the solvent. $CH_3NH_3PbI_3$ film prepared with BL/DMSO solvent shows a relative smooth surface. And such film presents a higher light absorption. I-V curves indicate that $CH_3NH_3PbI_3$ film prepared with BL/DMSO shows a superior photoelectrical performance. The hole transport kinetics is also discussed in the article.

2. EXPERIMENTS

2.1. Synthesis of $CH_3NH_3PbI_3$ (1) and $CH_3NH_3PbI_3$ (2)

CH_3NH_3I was prepared according to previous method [21]. $CH_3NH_3PbI_3$ (1) and $CH_3NH_3PbI_3$ (2) were prepared in nitrogen atmosphere glove box.

$CH_3NH_3PbI_3$ (1) prepared with DMAC/DMF solvent: CH_3NH_3I (0.159 g) and PbI_2 (0.461g) are dissolved in DMAC （0.9 ml）and DMF（0.1 ml）mixed solution. After stirring at 70℃ for 12h, the obtained solution was filtered.

$CH_3NH_3PbI_3$ (2) prepared with BL/DMSO solvent: CH_3NH_3I (0.159 g) and PbI_2 (0.461g) are dissolved in BL（0.7 ml） and DMSO（0.3 ml）mixed solution. After stirring at 70℃ for 12h, the obtained solution was filtered.

2.2. Photoelectrical performance

Doctor blade method was used to prepare photocathode NiO films in air. The first compact layer was prepared by coating NiO nanoparticles directly on FTO following with the second light scattering layer. The photocathode semiconductor films were calcined in air for 30 minutes at 500 ˚C and then transferred to nitrogen atmosphere glove box. The prepared $CH_3NH_3PbI_3$ (1) was spin-coated on the NiO film first at 800 rpm for 10 s, then 4000 rpm for 40 s during which 1 ml of toluene was dripped on the film. Then the $CH_3NH_3PbI_3$ (1) film was annealed at 100 ˚C for 5 minutes. A similar

manner was taken for $CH_3NH_3PbI_3$ (2) by only changing the time at 800 rpm to 90 s. The photocathodes and the platinized counter electrodes were sealed together by Surlyn film with electrolyte (0.5 M LiI, 0.05 M I_2 and 0.5 M 4-tertbutylpyridine in acetonitrile) injected. The effective area of p-DSSC was 0.25 cm^2. Photoelectrochemical and electrochemical impedance measurments are tested by Zahner CIMPS-2 workstation together with a Trusttech CHF-XM-500W source (Global AM 1.5, 100 mW cm^{-2}). The frequency range of EIS was from 100 kHz to 0.1 Hz with AC amplitude of 10 mV. Intensity-modulated photovoltage spectroscopy (IMVS) and intensity-modulated photocurrent spectroscopy (IMPS) were measured by Zahner CIMPS-2 workstation. 470 nm LED light was used as illumination driven by PP210 workstation. The frequency range of the test was from 1000 Hz to 0.01 Hz.

3. RESULTS AND DISCUSSION

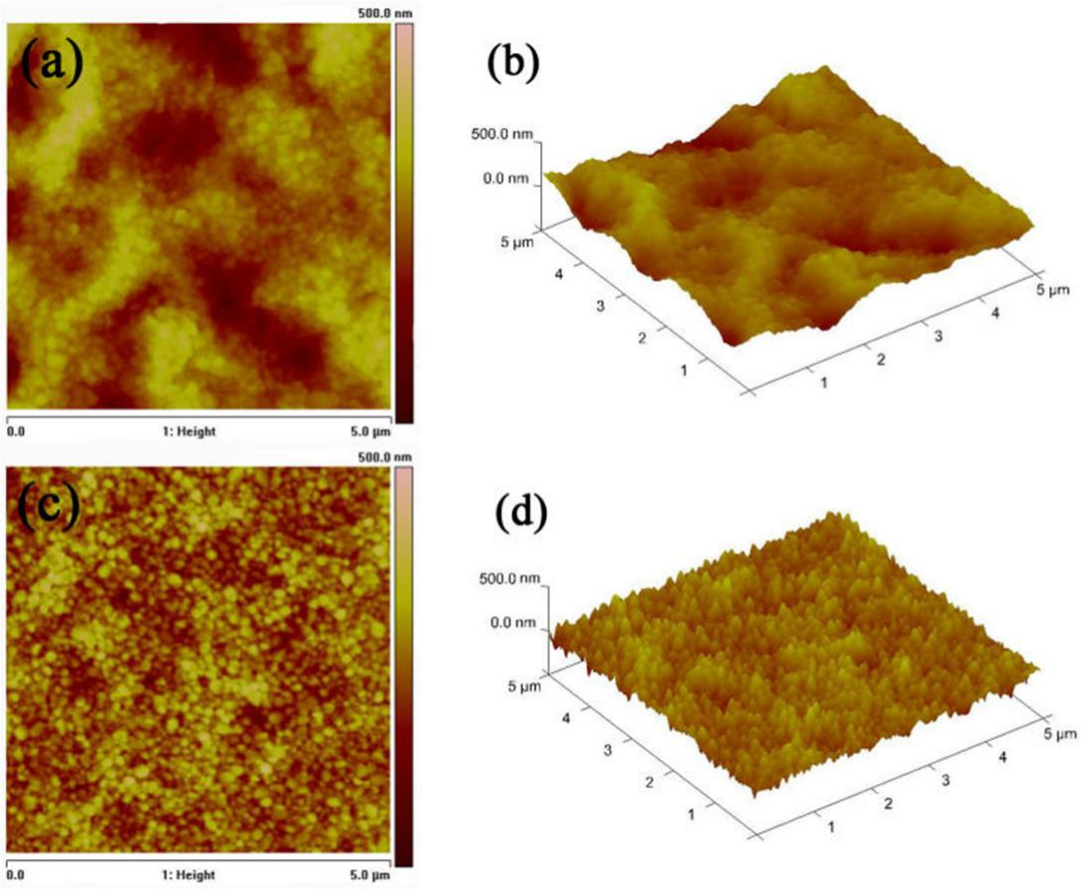

Figure 1. AFM two-dimensional images of 5 µm × 5 µm region of $CH_3NH_3PbI_3$ (1) thin film (a) and $CH_3NH_3PbI_3$ (2) (c); AFM three-dimensional images of $CH_3NH_3PbI_3$ (1) thin film (b) and $CH_3NH_3PbI_3$ (2) (d).

The surface topography information of $CH_3NH_3PbI_3$ films was examined by using atom force microscopy (AFM) as shown in Fig. 1. Bright and dark contrast indicates the protrusions and depressions of the $CH_3NH_3PbI_3$ films. It is clear from Fig. 1a and 1b that $CH_3NH_3PbI_3$ (1) shows an

obvious protrusion and depression of 403 nm, which indicate a not smooth surface. As a result the root-mean-square (RMS) roughness can reach up to 48 nm. Such wrinkle surfaces indicate more defects which could further hinder the hole transport and increase the recombination. When using BL/DMSO mixed solvent to prepare $CH_3NH_3PbI_3$, the roughness of the surface was greatly improved. Fig. 1c and 1d show a relative smooth surface with a slight protrusion and depression of 124 nm. And the root-mean-square (RMS) roughness was reduced to 12 nm. As we all know, solvent shows enormous influence in $CH_3NH_3PbI_3$ synthesis. The volatility of DMF is very fast, so using single DMF as the solvent is difficult to form a film. DMAC adding can slow the volatility which could be helpful for the film formation. But the quality of the film still need to be further improved. Using BL/DMSO solvent, we can easily get a relative high quality of $CH_3NH_3PbI_3$ film. DMSO shows a slow volatility and it may just prevent the formation of colloidal PbI_2 and lead to more uniform nucleation for $CH_3NH_3PbI_3$ formation. In addition, toluene added during spin-coating is used to stabilize the formation of CH_3NH_3I-PbI_2-DMSO complex, which is then converted to a smooth, continuous $CH_3NH_3PbI_3$ film by annealing [22].

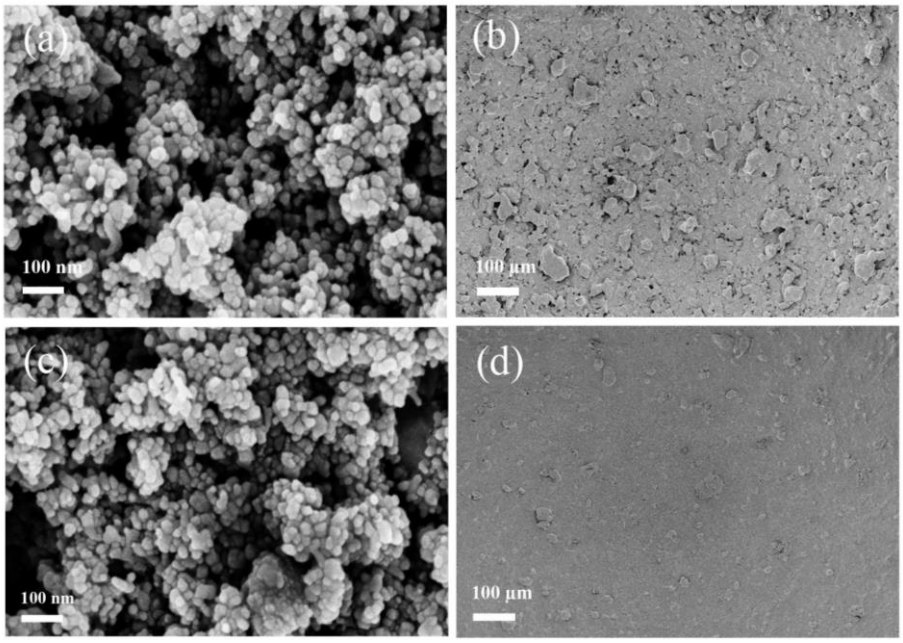

Figure 2. SEM images of $CH_3NH_3PbI_3$ (1)-sensitized NiO film with top view (a) and (b); SEM images of $CH_3NH_3PbI_3$ (2)-sensitized NiO film with top view (c) and (d).

Fig.2 shows the top view SEM images of $CH_3NH_3PbI_3$ (1) and $CH_3NH_3PbI_3$ (2)-sensitized mesoporous NiO film. It is clear that $CH_3NH_3PbI_3$ layer is coating on top of the mesoporous NiO film. But not all the pore channels of the NiO film are filled by CH_3NH_3PbI. As reported in previous article [5], $CH_3NH_3PbI_3$ sensitizers are absorbed on the surface of NiO nanoparticle in the form of thin shell or isolated nanocrystals or their mixture, which is consistent with the typical feature of conventional DSSCs and QDSCs. And they play the same role as the conventional dyes. It is no doubt that $CH_3NH_3PbI_3$ sensitizers show a good penetration and a homogeneous distribution. As seen from

Fig.2b, a rough and a serious protruded and depressed film surface is detected. However, the surface of $CH_3NH_3PbI_3$ (2) is much more smooth. These results are in consistent with AFM analysis. $CH_3NH_3PbI_3$ (2) with smooth surface would accelerate the hole transport and reduce the recombination following with an improved photoelectrical performance.

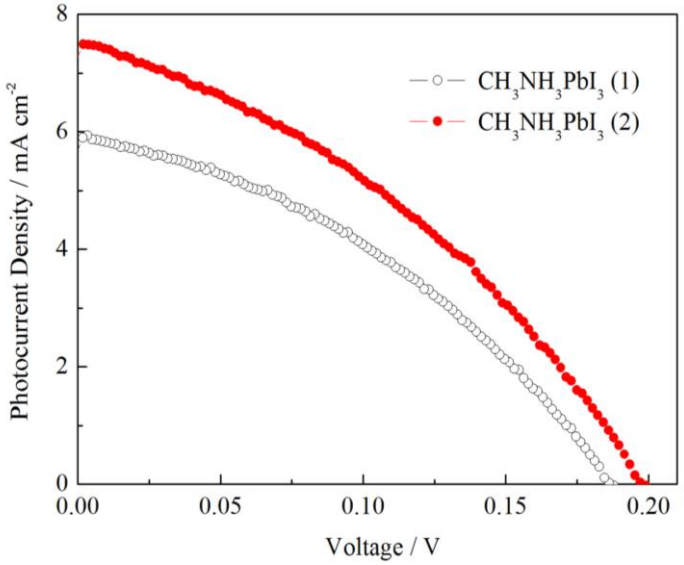

Figure 3. I-V curves for p-solar cells based on $CH_3NH_3PbI_3$ (1) and $CH_3NH_3PbI_3$ (2)-sensitized NiO photocathodes.

The photoelectrical performance of the solar cells with $CH_3NH_3PbI_3$ (1) and $CH_3NH_3PbI_3$ (2)-sensitized NiO photocathodes are shown in Fig. 3 and the measured and calculated values are summarized in Table 1. As shown in Fig. 3, $CH_3NH_3PbI_3$ (2) shows a higher short circuit current density (J_{sc}) of 7.5 mA cm^{-2}, while the J_{sc} of $CH_3NH_3PbI_3$ (1) is 5.9 mA cm^{-2}. An open circuit voltage (V_{oc}) of 197 mV is observed for $CH_3NH_3PbI_3$ (2), which is higher than that of $CH_3NH_3PbI_3$ (1). A conversion efficiency (η) of 0.53% is calculated for $CH_3NH_3PbI_3$ (2).

Table 1. The calculated details of p-DSSCs based $CH_3NH_3PbI_3$ (1) and $CH_3NH_3PbI_3$ (2)-sensitized NiO photocathodes.

	J_{sc} / mA cm^{-2}	V_{oc} / mV	*FF*	*η* / %
$CH_3NH_3PbI_3$ (1)	5.9	186	0.38	0.41
$CH_3NH_3PbI_3$ (2)	7.5	197	0.36	0.53

UV-vis absorption spectra of the NiO/$CH_3NH_3PbI_3$ films are shown in Fig.4. It is clear that thin films of NiO/$CH_3NH_3PbI_3$ (1) and NiO/$CH_3NH_3PbI_3$ (2) absorb a wide range of light from 370 to 760 nm with a shoulder band at about 450-500 nm, which is in line with former reports [23-25]. And for NiO/$CH_3NH_3PbI_3$ (2), the range of absorption can reach up to 1000 nm, even though the absorption

from 760 nm to 1000 nm is low. In general, NiO/$CH_3NH_3PbI_3$ (2) shows higher absorption than NiO/$CH_3NH_3PbI_3$ (1), which can be attributed to the higher quality of the $CH_3NH_3PbI_3$ (2) film. The above results also indicate a relatively more photons absorption for $CH_3NH_3PbI_3$ (2) following with improved short circuit current density, open circuit voltage and conversion efficiency. This is consistent with the I-V results.

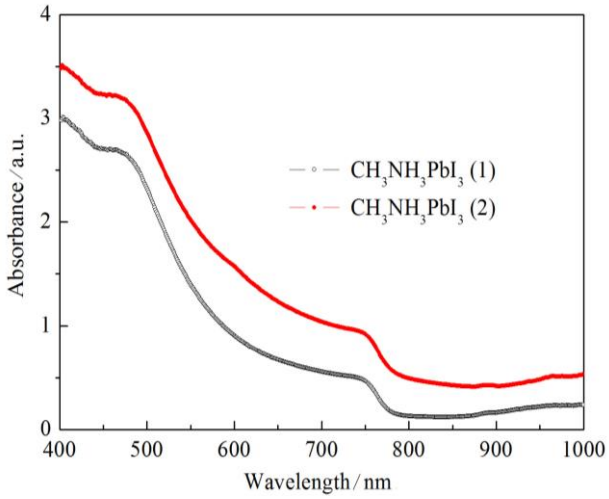

Figure 4. UV-vis absorption spectra of FTO/NiO/$CH_3NH_3PbI_3$ (1) and FTO/NiO/$CH_3NH_3PbI_3$ (2) films.

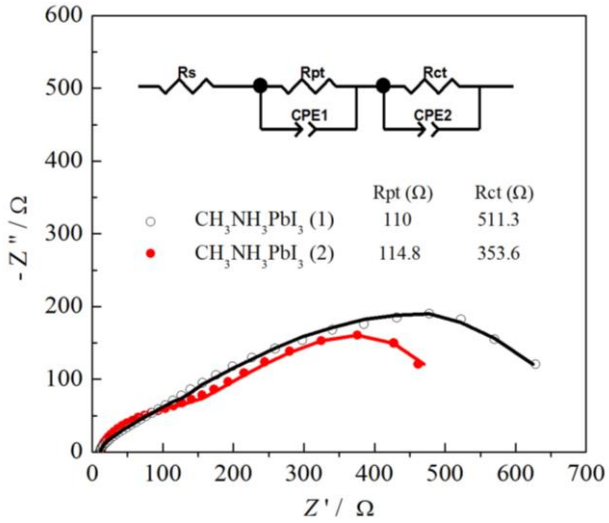

Figure 5. EIS measurments, equivalent circuit and fitted data of solar cells based on $CH_3NH_3PbI_3$ (1) and $CH_3NH_3PbI_3$ (2)-sensitized NiO photocathodes.

Fig. 5 shows the electrochemical impedance spectra (EIS) of p-DSSCs with $CH_3NH_3PbI_3$ (1) and $CH_3NH_3PbI_3$ (2)-sensitized NiO photocathodes. Seen from EIS plots, there are two semicircles. The left semicircle could be corresponded to the Pt counter electrode interface hole transfer (R_{pt}) process. And the right semicircle can be assigned to the NiO/$CH_3NH_3PbI_3$/electrolyte interface (R_{ct})

hole-transfer process [26]. The R_{pt} values estimated from the diameter of the semicircle for the two samples are almost the same, much lower than the corresponding R_{ct} values. And the R_{ct} values of two samples are clearly different with $CH_3NH_3PbI_3$ (2) smaller than $CH_3NH_3PbI_3$ (1). The comprehensive fitting results of this Nyquist plots [27] are summarized in Fig. 5 inset. The total resistance of $CH_3NH_3PbI_3$ (2) is much lower than that of $CH_3NH_3PbI_3$ (1), which means a superior hole transport kinetics following with an improved photoelectrical performance. Such results are in agreement with I-V curve discussed above.

Intensity-modulated photocurrent spectroscopy (IMPS) and intensity-modulated photovoltage spectroscopy (IMVS) are tested for further investigating the hole kinetics. Table 2 shows the calculated details of the two spectroscopies [26, 28]. The hole transport time (τ_{tr}) of $CH_3NH_3PbI_3$ (2) is a little smaller than $CH_3NH_3PbI_3$ (1), which may contribute to the high quality of $CH_3NH_3PbI_3$ (2) film. And the hole life time (τ_h) of $CH_3NH_3PbI_3$ (2) is longer than that of $CH_3NH_3PbI_3$ (1) and the τ_h/τ_{tr} ratio of $CH_3NH_3PbI_3$ (2) is bigger than that of $CH_3NH_3PbI_3$ (1). Such results indicate a fast hole transport and less recombination for $CH_3NH_3PbI_3$ (2) cells. The charge collection efficiency η_{cc} ($\eta_{cc} = 1-\tau_{tr}/\tau_h$) of the two samples are calculated [29]. It is no doubt that $CH_3NH_3PbI_3$ (2) shows higher charge collection efficiency, which can be contributed to the fast transport and less recombination. The hole diffusion coefficient can be estimated by $D = d^2/2.35\tau_{tr}$, where d is the film thickness [30]. D values of the two samples are still very low as reported previously in p-DSCs in the range of 10^{-7}-10^{-6} cm^2 s^{-1} [31], which is still a big problem for p-DSSCs and need further research.

Table 2. Calculated details of the p-DSSCs based on $CH_3NH_3PbI_3$ (1) and $CH_3NH_3PbI_3$ (2)-sensitized NiO photocathodes for IMPS and IMVS.

	τ_{tr} / ms	τ_h / ms	η_{cc}	D / cm^2 s^{-1}
$CH_3NH_3PbI_3$ (1)	20	39	0.49	8.5×10^{-7}
$CH_3NH_3PbI_3$ (2)	18	40	0.55	9.4×10^{-7}

4. CONCLUSIONS

In conclusion, organometal halide perovskite $CH_3NH_3PbI_3$ sensitizers have been prepared with two different mixed solvents, dimethylacetamide/dimethylformamide (DMAC/DMF) (1) and butyrrolactone/dimethyl sulphoxide (BL/DMSO) (2), which show great influence on the quality of the $CH_3NH_3PbI_3$ films. Using BL/DMSO, $CH_3NH_3PbI_3$ film presents a superior surface. A smooth surface with slight protrusion and depression of 124 nm and roughness of 12 nm was obtained. UV-vis absorption spectra indicate that $CH_3NH_3PbI_3$ (2) shows higher light absorption than $CH_3NH_3PbI_3$ (1). I-V curve indicates that $CH_3NH_3PbI_3$ (2) shows a higher J_{sc} of 7.5 mA cm^{-2}. And a higher efficiency of 0.53% was also obtained. Besides, $CH_3NH_3PbI_3$ (2) with a high quality film shows fast hole transport, less recombination and improved conversion efficiency.

ACKNOWLEDGMENTS
This work has been supported by the National Natural Science Foundation of China (21301022), Major Projects of Natural Science Research in Jiangsu Province (15KJA43002) and the Project Funded by China Postdoctoral Science Foundation (2015M571633).

References

1. J. He, A. Hagfeldt, S. E. Lindquist, *Sol. Energy Mater. Sol. Cells*, 62 (2000) 265-273.
2. S. Powar, T. Daeneke, M. T. Ma, D. Fu, N. W. Duffy, G. Goetz, M. Weidelener, A. Mishra, P. Baeuerle, L. Spiccia, U. Bach, *Angew. Chem., Int. Ed*, 52 (2013) 602-605.
3. X. L. Zhang, Z. Zhang, D. Chen, P. Bäuerle, U. Bache, Y. B. Cheng, *Chem. Commun*, 8 (2012) 9885-9887.
4. D. Xiong, H. Wang, W. Zhang, X. Zeng, H. Chang, X. Zhao, W. Chen, Y. B. Cheng, *J. Alloy. Compd*, 642 (2015) 104-110.
5. Y. Mizoguchi, S. Fujihara, *Electrochem. Solid. ST*, 11 (2008) K78-K80.
6. H. Wang, X. Zeng, Z. Huang, W. Zhang, X. Qiao, B. Hu, X. Zou, M. Wang, Y. B. Cheng, W. Chen, *ACS Appl. Mater. Interfaces*, 6 (2014) 12609-12617.
7. P. Qin, H. Zhu, T. Edvinsson, G. Boschloo, A. Hagfeldt, L. Sun, *J. Am. Chem. Soc*, 130 (2008) 8570-8571.
8. Z. Liu, W. Li, S. Topa, X. Xu, X. Zeng, Z. Zhao, M. Wang, W. Chen, F. Wang, Y. B. Cheng, H. He, *ACS Appl. Mater. Interfaces*, 6 (2014) 10614-10622.
9. L. L. Sun, T. Zhang, J. Wang, H. Li, L. K. Yan, Z. M. Su, *RSC Adv*, 5 (2015) 39821-39827.
10. S. H. Kang, K. Zhu, N. R. Nealeb, A. J. Frank, *Chem. Commun*, 47 (2011) 10419-10421.
11. S. Mori, S. Fukuda, S. Sumikura, Y. Takeda, Y. Tamaki, E. Suzuki, T. Abe, *J. Phys. Chem. C*, 112 (2008) 16134-16139.
12. A. Morandeira, G. Boschloo, A. Hagfeldt, L. Hammarstrom, *J. Phys. Chem. B*, 109 (2005) 19403-19410.
13. H. Zhu, A. Hagfeldt, G. Boschloo, *J. Phys. Chem. C*, 111 (2007) 17455-17458.
14. A. Morandeira, G. Boschloo, A. Hagfeldt, L. Hammarstrom, *J. Phys. Chem. C*, 112 (2008) 9530-9537.
15. A. Morandeira, J. Fortage, T. Edvinsson, L. Le Pleux, E. Blart, G. Boschloo, A. Hagfeldt, L. Hammarstrom, F. Odobel, *J. Phys. Chem. C*, 112 (2008) 1721-1728.
16. E. A. Gibson, A. L. Smeigh, L. Le Pleux, J. Fortage, G. Boschloo, E. Blart, Y. Pellegrin, F. Odobel, A. Hagfeldt, L. Hammarstrom, *Angew. Chem., Int. Ed*, 48 (2009) 4402-4405.
17. M. Borgstrom, E. Blart, G. Boschloo, E. Mukhtar, A. Hagfeldt, L. Hammarstromand, F.Odobel, *J. Phys. Chem. B*, 109 (2005) 22928-22934.
18. P. Qin, M. Linder, T. Brinck, G. Boschloo, A. Hagfeldt, L. Sun, *Adv. Mater*, 21 (2009) 2993-2996.
19. P. Qin, J. Wiberg, E. A. Gibson, M. Linder, L. Li, T. Brinck, A. Hagfeldt, B. Albinsson, L. Sun, *J. Phys. Chem. C*, 114 (2010) 4738-4748.
20. A. Nattestad, A. J. Mozer, M. K. R. Fischer, Y. B. Cheng, A. Mishra, P. Bäuerle, U. Bach, *Nat. Mater*, 9 (2010) 31-35.
21. P. W. Liang, C. Y. Liao, C. C. Chueh, F. Zuo, S. T. Williams, X. K. Xin, J. Lin, A. K. Y. Jen, *Adv. Mater*, 26 (2014) 3748-3754.
22. N. J. Jeon, J. H. Noh, Y. C. Kim, W. S. Yang, S. Ryu, S. I. Seok, *Nat. Mater*, 13 (2014) 897-903.
23. J. Chang, H. Zhu, B. Li, F. H. Isikgor, Y. Hao, Q. Xu, J. Ouyang, *J. Mater. Chem. A*, 4 (2016) 887-893.
24. Q. Zhu, X. Bao, J. Yu, D. Zhu, M. Qiu, R. Yang, L. Dong, *ACS Appl. Mater. Interfaces*, 8 (2016) 2652-2657.

25. J. W. Jung, C. C. Chueh, A. K. Y. Jen, *Adv. Mater*, 27 (2015) 7874-7880.
26. Z. Huang, G. Natu, Z. Ji, M. He, M. Yu, Y. Wu, *J. Phys. Chem. C*, 116 (2012) 26239-26246.
27. J. Qu, X. P. Gao, G. R. Li, Q. W. Jiang, T. Y. Yan, *J. Phys. Chem. C*, 113 (2009) 3359-3363.
28. J. Qu, G. R. Li, X. P. Gao, *Energy Environ. Sci*, 3 (2010) 2003-2009.
29. S. D. Stranks, G. E. Eperon, G. Grancini, C. Menelaou, M. J. P. Alcocer, T. Leijtens, L. M. Herz, A. Petrozza, H. J. Snaith, *Science*, 342 (2013) 341-344.
30. Y. Zhao, K. Zhu, *J. Phys. Chem.Lett*, 4 (2013) 2880-2884.
31. Z. Xu, D. Xiong, H. Wang, W. Zhang, X. Zeng, L. Ming, W. Chen, X. Xu, J. Cui, M. Wang, S. Powar, U. Bach, Y. B. Cheng, *J. Mater. Chem. A*, 2 (2014) 2968-2976.